PNNL-33334

Light Water Reactor Sustainability Program

Nondestructive Evaluation (NDE) of Cable Anomalies using Frequency Domain Reflectometry (FDR) and Spread Spectrum Time Domain Reflectometry (SSTDR)

September 2022

U.S. Department of Energy

Office of Nuclear Energy

PNNL-33334

Nondestructive Evaluation (NDE) of Cable Anomalies using Frequency Domain Reflectometry (FDR) and Spread Spectrum Time Domain Reflectometry (SSTDR)

S.W. Glass, A. Sriraman, M. Prowant, M.P. Spencer, L.S. Fifield
Pacific Northwest National Laboratory

S. Kingston
LiveWire Innovation, Inc.

September 2022

Prepared for the
U.S. Department of Energy
Office of Nuclear Energy

SUMMARY

This report presents a comparative assessment of the performance of frequency domain reflectometry (FDR) and spread spectrum time domain reflectometry (SSTDR) in detecting a wide range of electrical cable anomalies. All tests and results reported herein were performed at the PNNL Accelerated and Real-Time Environmental Nodal Assessment (ARENA) cable and motor test bed developed for cable/motor NDE. The primary objective of this work was to evaluate the effectiveness of SSTDR, a fledgling cable monitoring technique that shows promise for application in online monitoring of energized cable systems, against FDR, an offline technique widely employed in the nuclear power plant (NPP) industry.

FDR tests are becoming more widely used in nuclear power plant cable aging management and test programs – particularly for low voltage cables. FDR capabilities for these kinds of tests have been reported by PNNL and others. The FDR test is performed on de-energized cables by connecting the FDR instrument to two of the cable conductors, or one conductor and the shield. A broad-band low voltage (< 5 V) chirp is introduced in the cable and any reflected response is captured in the frequency domain. The captured reflection is then processed by performing an inverse Fourier transform to a time domain response which can then be converted to a distance response based on the cable velocity of propagation (VoP, normally provided as fraction of the speed of light). SSTDR measurements are functionally similar to FDR measurements in that a broad-band voltage signal composed of a square or sine wave modulated pseudo-random sequence of chirps (< 5 volts) is injected onto one of the cable conductors. The injected signal will experience partial energy reflection and transmission at each impedance discontinuity along the transmission line. Any reflected response is detected by computing a cross-correlation between the reflected signals and a delayed copy of the incident SSTDR signal. The time delay for the reflected signal to experience the best matched correlation with the incident signal indicates travel time for the signal to reach a change in impedance. By knowing this time delay and VoP of the signal, one can compute the physical distance. A significant advantage that SSTDR measurements have over other methods is the ability to be connected to energized or live wires (currently up to 1kV) thereby enabling online monitoring of cables. SSTDR has been used successfully in several applications, e.g., aircraft, rail, and photovoltaic systems.

In this work FDR and SSTDR cable assessment techniques were used to characterize a variety of cable anomalies and faults including:

(1) Presence or absence of a motor;

(2) Ground faults and short circuit faults;

(3) Moist environments and water ingress faults; and

(4) Accelerated thermal aging.

Both shielded and non-shielded cables were evaluated in this report. Offline measurements were made using FDR and online measurements were made by SSTDR for a range of test scenarios. Based on the results across all cable anomalies evaluated in this study, FDR displayed high sensitivity (clearer peaks above baseline noise) towards cable condition assessment, while SSTDR showed promise for future application in monitoring NPP cable systems. However, further developments (like increased bandwidth) are suggested to improve the resolution and sensitivity of SSTDR towards faults and anomalies in low voltage cables.

ACKNOWLEDGEMENTS

This work was sponsored by the U.S. Department of Energy (DOE), Office of Nuclear Energy, for the Light Water Reactor Sustainability (LWRS) Program Materials Research Pathway. The authors extend their appreciation to Pathway Lead Dr. Thomas Rosseel for LWRS programmatic support. This work was performed at the Pacific Northwest National Laboratory (PNNL). PNNL is operated by Battelle for the U.S. DOE under contract DE-AC05-76RL01830. The SSTDR work was led by LiveWire Innovation Inc., supported by PNNL, and sponsored under DOE award number DE-SC0021816.

CONTENTS

FIGURES

TABLES

ACRONYMS

AMP	Aging Management Program
AMS	Analysis and Measurement Services
ARENA	Accelerated and Real-Time Environmental Nodal Assessment
ASIC	application-specific integrated circuit
AWG	American wire gauge
c	speed of light or 299,792,458 m/s
CPE	chlorinated polyethylene
DBE	design-basis event
EAB	elongation at break
EPR	ethylene propylene rubber
EPRI	Electric Power Research Institute
FDR	frequency domain reflectometry
FFT	fast Fourier transform
HV	high voltage
LOCA	loss-of-coolant accident
LV	low voltage
LWRSP	Light Water Reactor Sustainability Program
MCR	multicarrier reflectometry
MSR	mixed signal reflectometry
NDE	nondestructive evaluation
NPP	nuclear power plant
NRC	U.S. Nuclear Regulatory Commission
PNNL	Pacific Northwest National Laboratory
PVC	polyvinyl chloride
RF	radio frequency
SLR	subsequent license renewal
SSTDR	spread spectrum time domain reflectometry
S/SSTDR	sequence/spread spectrum time domain reflectometry
SWR	standing wave reflectometry
TDR	time domain reflectometry
TEM	transverse electromagnetic
VNA	vector network analyzer
VoP	velocity of propagation

1. INTRODUCTION

This report is submitted in fulfillment of the deliverable for the LWRS milestone (M3LW-22OR0404023) for NDE of cables and cable insulation. This work is part of an overall project to develop a technical basis for assessing the level and impact of cable insulation aging and degradation in nuclear power plants (NPPs). In July 2012, a workshop was held at PNNL to lay the groundwork for a research and development roadmap to address aging cable management in NPPs particularly focused on nondestructive examination (Simmons et al., 2012). Following this, PNNL has developed capabilities for thermal, radiation, and combined thermal and radiation aging of cables. Furthermore, significant capabilities to test, monitor, and evaluate cable conditions have been developed (Fifield et al., 2015; Glass S.W. et al., 2015; Glass et al., 2016; Glass et al., 2017; Glass et al., 2018; Glass, Fifield, and Bowler, 2020; Glass S.W., 2021). The work described herein investigates a large variety of cable faults to further support the overall project objectives to monitor cable insulation aging and failure.

In this section, the motivation for the work is first introduced, followed by relevant background and literature. Finally, the objectives of this study and a brief outline of the contents of this report are detailed.

1.1 Motivation

Most of the NPPs currently operating in the United States are approximately 35 to 55 years old, and many are preparing for subsequent license renewals (SLRs) to extend their operating periods by another 20 years (NRC, 2021). A critical step towards continued safe operation of NPPs during extended license periods is to evaluate how the characteristics and performance of materials installed in aging plant components will change over time. This, in turn, informs the development of aging management programs to ensure continued safe operation under normal and design-basis events (DBE).

Given the large volume of different types of cables servicing NPPs, prevention and detection of cable failure during the operating lifetime of an NPP is a vital part of aging management. As such, most NPPs now have cable management programs that implement nondestructive evaluation (NDE) to determine electrical cable performance. While NDE techniques have seen growth and improvement in cable diagnostics and fault detection performance, practical implementation of NDE has a few limitations. First, there is no single NDE method to comprehensively evaluate cable performance and safety, and therefore a combination of multiple global and local tests are required to collectively provide a high reliability assessment of cable performance (Glass S.W. et al., 2015). Second, most of the widespread NDE techniques (reflectometry, dielectric spectroscopy (DS), tan delta, etc.) require cables to be powered down and/or disconnected on at least one end to implement the test, which may ultimately result in higher operation and maintenance costs. Consequently, to improve the efficiency and cost-effectiveness of cable testing, utilities are constantly on the lookout for alternative ways to implement fewer and more robust NDE techniques for cable assessment. Two initiatives that help manage time and costs are i) online monitoring (i.e., NDE on live or energized cables), and ii) employment of NDE techniques that can be implemented even with a motor attached. The transition to online monitoring for real-time cable assessment lowers costs associated with the significant down time caused by de-energizing and disconnecting the cable system to perform the test. Similarly, implementing NDE tests that can be performed while leaving the motor connected helps minimize disconnect and re-connect costs. In this context, research studies and pilot-scale evaluations of the efficacy of fledgling NDE technologies that exhibit potential for reduced costs and higher efficiency is an invaluable step towards future implementation of these technologies in NPPs.

This report seeks to evaluate and compare the performance of a fledgling NDE technique that shows promise in overcoming the aforementioned limitations against a more widespread and well-established conventional cable NDE technique, to provide an initial assessment of the state of the art. The former is spread spectrum time domain reflectometry (SSTDR), an NDE approach that can be implemented i) on live

or energized cables, and ii) without requiring cable or motor disconnection; while the latter is frequency domain reflectometry (FDR), a broadly implemented NDE approach, which typically requires i) cables to be de-energized, and ii) cable disconnection on at least one end. In the following section, a brief overview of reflectometry techniques is provided followed by a literature review of recent developments in FDR and SSTDR measurement methods.

1.2 Background

Broadly, reflectometry is a non-destructive technique that is based on the reflection of electromagnetic waves at surfaces and/or interfaces to locate changes and characterize various objects. Within the realm of electrical characterization, reflectometry techniques may be applied to nondestructively conduct distance-to-fault (DTF) measurements on electrical cables and wires. Based on the type of input signal used and the method for analysis of the reflected signal, reflectometry techniques applied for cable evaluations may be broadly categorized as FDR or time domain reflectometry (TDR). For FDR measurements, the steady-state amplitude and phase of the reflected signal is built up over numerous discrete frequencies, while for TDR signals, the reflected signal is measured at discrete moments in time.

1.2.1 Frequency Domain Reflectometry (FDR)

FDR is a nondestructive electrical inspection technique used to detect, localize, and characterize subtle impedance changes in power and communication system conductors and insulation materials along the length of a cable from a single connection point. FDR is based on the interaction of electromagnetic waves with conductors and dielectric materials as the waves propagate along the cable. The technique uses the principles of transmission line theory to locate and quantify impedance changes in the cable circuit. These impedance changes can result from connections, faults in the conductors, or degradation in the cable insulation material (Furse et al., 2003; Agilent, 2012).

For an FDR measurement, two conductors in the cable system are treated as a transmission line through which a low-voltage swept-frequency waveform is propagated. A linearly increasing “chirp” sinusoidal waveform is the typical excitation signal used in the FDR technique. The excitation signal can be generated for transmission into the cable using an analog circuit, such as a voltage-controlled oscillator, or using a digital circuit such as a direct digital synthesizer. As the excitation signal is swept over the frequency range and the associated electromagnetic wave travels down the cable, the impedance response is recorded at each frequency to characterize wave interaction with the conductors and surrounding dielectric materials. The remote end of the cable can be terminated in an arbitrary impedance different from the cable characteristic impedance but is often grounded or open-circuited during testing. Because the applied signal is low-voltage, the test is nondestructive and poses no special safety concerns to operators assuming that routine electrical safety procedures are followed (Glass et al., 2017). In most cases, it is only necessary to de-energize the cables and de-termination is not required, but typically at least one end of the cabling is de-terminated to connect the FDR system. De-terminating only one cable end can be an advantage over many other techniques by shortening the required testing time and minimizing the risk of improper re-termination. Frequently, however, both ends of the cable systems are de-terminated anyway to minimize the risk of residual charge shock and in some cases, reduce noise on the FDR signal.

1.2.2 Spread Spectrum Time Domain Reflectometry (SSTDR)

SSTDR is a combination of spread spectrum (SS) and TDR techniques. While TDR is a widely used technology for fault detection in cables and wires, spread spectrum finds extensive application in cellular technology. SSTDR is one of several enhancements to the traditional TDR measurement that are available today for locating electrical faults based on reflectometry concepts. These include standing wave reflectometry (SWR), mixed signal reflectometry (MSR) (Tsai P., 2005), multicarrier reflectometry (MCR)

(Naik S., 2006) and sequence/spread spectrum time domain reflectometry (S/SSTDR) (Smith P., 2008). For online applications, S/SSTDR has been most fully exploited in the aircraft industry and the rail industry where low-cost ASIC-based instruments have been developed for online monitoring of control and power circuits up to 1000 volts.

SSTDR in particular shows promise as a robust online cable monitoring technique owing to its unique ability to operate on energized cable systems. This feature is in sharp contrast with traditional reflectometry methods that require cables to be de-energized and de-terminated prior to testing. Similar to conventional reflectometry, SSTDR sends an excitation signal down the length of the cable and an analysis of the reflected signal is carried out to identify impedance discontinuities in the cable corresponding to faults and anomalies. One key difference lies in the type of signal used in SSTDR testing. SSTDR uses a high frequency pseudo-random-noise (PN) coded excitation signal that reflects off impedance discontinuities in the cable. The PN code effectively distributes the energy of the input signal across a broad spectrum (hence the name, spread spectrum), resulting in the signal traveling through the cable with little to no interference at any individual frequency in an energized cable. The reflected signal is then cross correlated with the input signal to produce a reflectometry spectrum. Another key advantage of SSTDR in contrast to TDR or FDR is that the instrument is designed to withstand 1000 volts thereby enabling the system to be applied to low voltage energized systems. A schematic representation of the SSTDR testing process is shown in Figure 1-1. While SSTDR has found application in aircraft and railway industries, the technology is in the developmental stages for application in the NPP industry. Evaluation of SSTDR performance against trusted cable monitoring technologies is critical for further development and eventual application of SSTDR to monitor energized cables in service in NPPs.

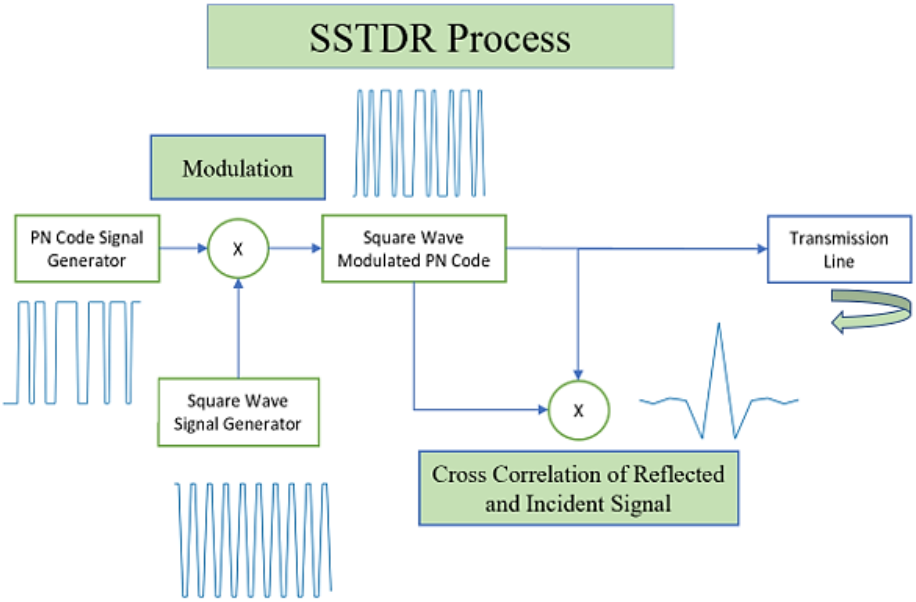

Figure 1-1. Schematic representation of SSTDR signal generation and analysis method.

1.3 Objectives

The primary goal of this work was to investigate the effectiveness of detecting a wide range of cable anomalies using two nondestructive test methods; FDR implemented offline (i.e., cable is de-energized) and SSTDR implemented online (i.e., cable is energized). To achieve this, the following objectives were developed:

(1) **Establish new capabilities for cable R&D**: Develop robust pilot-scale infrastructure at the ARENA test bed to perform a broad spectrum of cable monitoring and anomaly detection studies.

(2) **Investigate the effects of motor connection**: for shielded and non-shielded low-voltage (LV) cables using FDR and SSTDR. (Note that shielded and non-shielded cables have different electromagnetic field profiles that can result in different NDE results for the two types of cable).

(3) **Study cable anomalies**: Study the success of FDR and SSTDR techniques in pinpointing the nature and location of (i) ground faults and short circuit faults, and (ii) water ingress faults, in shielded and non-shielded LV cables.

(4) **Continuously monitor cable aging**: Evaluate the effectiveness of FDR and SSTDR techniques for real-time condition assessment of a non-shielded LV cable undergoing accelerated thermal aging.

In this report, first, the ARENA test bed infrastructure development is reported. Following this, the materials and experimental methods implemented are discussed. Next, test scenarios and corresponding results are detailed. Finally, the major findings and conclusions of this study are presented.

2. ARENA Test Bed Development

The key motivator for the establishment of the Accelerated and Real-Time Environmental Nodal Assessment (ARENA) test bed is that utilities are seeking lower cost, well-characterized, and reliable test methods to evaluate cables for service. Prior to implementation of any test method, it is important for utilities to verify that cable flaws are detected with an acceptable false-call ratio. The sheer volume of promising test methods for cable evaluation poses a major challenge for power utilities to identify and commit to any given testing strategy. In response to this challenge, targeted studies towards cable fault detection in a controlled environment provide a baseline understanding of the effectiveness of any given test method prior to trial examinations in the field. This fundamental investigation of test methods for pinpointing cable faults is an essential first step towards reliable fault detection in notoriously complex NPP cable systems.

To conduct rigorous and versatile cable studies using various test methods in a pilot-scale research environment, PNNL established the ARENA test bed in 2021 (see Figure 2-1). The vision behind the creation of this facility was to establish a one-stop modular test facility that allows for implementation of a broad range of test methods to detect faults and anomalies in a variety of cables and systems in a controlled environment. The goal is to assess the effectiveness of cable diagnostic and monitoring techniques safely and reliably in scenarios of interest to utilities, such as high-stress environments: elevated temperatures, electrical failures, moisture ingress, and more. As shown in Figure 2-1, the ARENA test bed features:

- A 3-phase 480 VAC motor that can be connected and run with either shielded or unshielded cables [the system is more fully described in (Glass, Fifield, and Prowant, 2021)];
- Cable taps for instruments both near the controller and near the motor;
- High sensitivity ground-fault circuit breaker technology to protect the line circuit breaker from faults in the cable and motor test bed;
- Remote control start/stop to protect operators from potential arc-flash hazards;
- A large thermal aging oven with inlet and outlet ports for thermal aging studies;
- A water trough to facilitate moisture ingress tests; and
- Elevated cable trays for personnel safety and to minimize cable movement during long-term tests.

All the tests and results presented within this report were conducted at the ARENA test bed facility.

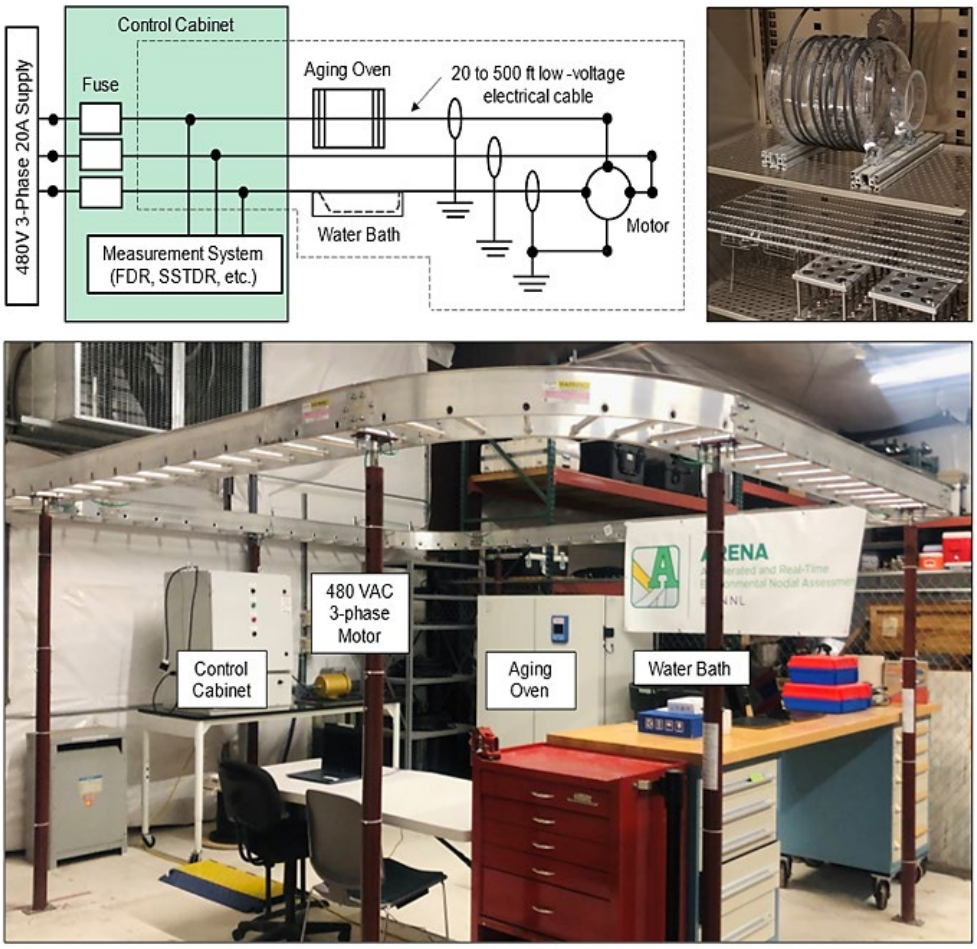

Figure 2-1. Digital image and schematic of the ARENA cable and motor test bed at PNNL.

3. Cable Anomaly Studies

As described in the objectives, this work included the evaluation of various cable anomalies using FDR and SSTDR techniques in the ARENA test bed. Specifically, the following test scenarios were evaluated:

(1) Motor connection or disconnection on shielded and non-shielded cables;

(2) Ground faults and line-to-line (short circuit) faults in shielded and non-shielded cables;

(3) Water ingress faults in shielded and non-shielded cables;

(4) Accelerated thermal aging studies in a non-shielded cable.

The setup for each of the test scenarios listed above is described in the next section alongside the results for ease of interpretation. In this section, the cables evaluated in this report are described, and the implemented test protocols and characterization methods are detailed. Furthermore, the overall test setup for the various cable anomalies is presented.

3.1 Materials

Low voltage, tri-core, shielded and non-shielded cables manufactured by General Cable® (Catalog number 383830) were chosen for this study. The overall specifications for the selected cables are given in Table 1. Both shielded and non-shielded cable variants were comprised of three 14 AWG conductor wires

insulated by ethylene propylene rubber (EPR) and protected by a chlorinated polyethylene (CPE) jacket. Additionally, the shielded cable contains an aluminum foil shield layer between the jacket and insulated wires. The cables have a voltage rating of 600 V and an operating temperature rating of 90 °C. All FDR and SSTDR tests were performed on cables of around 100 ft length.

Table 1. Manufacturer information for the cables selected for evaluation.

Manufacturer	P/N	Jacket	Insulation	Type
General Cable	354800	CPE	EPR	Shielded
	6-903-SH 14AWG-3/C FR-EP 600V FR-EPR/CPE Foil Shielded 600V E-2			
General Cable	383830	CPE	EPR	Non-Shielded
	6-903-G 14AWG-3/C FR-EP 600V FR-EPR/CPE Non-Shld 600V E-2			

EPR = ethylene-propylene rubber; CPE = chlorinated polyethylene.

3.2 Experimental Methods

A compact vector network analyzer (VNA) manufactured by Copper Mountain (2020) was used to perform FDR measurements (Copper Mountain, 2020). The frequency bandwidth for the FDR chirp signal was 300 kHz to 100 MHz for aging and electrical fault studies, and 300 kHz to 500 MHz for water ingress studies to accommodate the desired spatial resolutions of 3.3 ft and 0.6 ft, respectively. The velocity factor for the cable was set at 0.66 and the number of frequency samples was 1,024 to ensure signal propagation down the entire length of the cable at all chosen bandwidths. For each FDR measurement, two of the three conductor leads of the cable were randomly selected and attached to the VNA for measurement using alligator clips. Once chosen, the same two leads were applied for all tests in a given experiment. Care was taken to minimize any impedance mismatch during testing. All FDR measurements were made on the de-energized (offline) cables only. The collected FDR data was then processed using Microsoft Excel wherein the data was converted to the time domain using inverse Fourier transform without any zero padding. The magnitude of the reflection coefficient of the FDR signal was then plotted against the length along the cable.

The SSTDR test device implemented in this report is a patented technology manufactured by Livewire Innovation Inc. The test device comprised an SSTDR module that generates the test signal and a fault trapper that allows for the SSTDR device to 'T' into the cable under test while it is energized. The frequency bandwidth of the applied SSTDR signal was 0 – 48 MHz with the center frequency (i.e., the frequency with the maximum intensity) at 24 MHz. After injection, the reflected signal from the cable was cross correlated with a copy of the original input signal to obtain the impedance discontinuities along the length of the cable using a proprietary software developed by Livewire Innovation Inc. The velocity of propagation (VoP) of the signal through the cable was set at 0.66 and was used to determine the distance along the cable where the impedance discontinuities were located. To ensure that the SSTDR measurements conducted on the cable were closely comparable to FDR measurements, the two leads chosen for FDR measurements were tested under identical conditions using SSTDR. The only difference being that many of the SSTDR measurements reported herein were conducted on the energized (online) cables.

Mechanical tensile tests were performed specifically to support cable aging studies (see Section 4.4). Cable insulation witness samples of 50 mm length (without the conductor) were extracted from cable segments and tested to track insulation degradation with thermal aging. Tensile tests were performed using an Instron 3367 extended travel instrument with a 30 kN load cell and pneumatic grips. The witness samples were tested in accordance with (IEEE, 2019) standard method. Tests were performed using a strain rate of 20 mm/min, gauge length of 20 mm, grip pressure of 40 psi, and grip separation of 30 mm. The insulation straws had an O.D. of 3.4 mm and thickness of 1 mm. Thermoplastic polyurethane (TPU) cylindrical end tabs of length 6 mm, O.D. 5.5 mm, and thickness 2 mm were applied on either end of each test specimen

prior to testing to ensure uniform load distribution and minimize damage from the grips. All measurements were performed at 22°C.

4. Results and Discussion

In this section, FDR and SSTDR responses for the cables under study in each of the test scenarios evaluated in this report are presented. The test setup is briefly described, and a schematic representation of the cable pathway is provided to allow for direct correlation with the results observed. Finally, the success of the FDR and SSTDR detection methods in pinpointing the locations of cable anomalies is discussed.

4.1 Motor Connection/Disconnection Detection

Figure 4-1. Schematic representation of the cable route for motor connection/disconnection test.

To investigate the influence of the presence or absence of a motor on the FDR and SSTDR responses of shielded and non-shielded cables, a simple test protocol was developed using a 480 VAC motor. A schematic representation of the test setup is shown in Figure 4-1. With one end of the cable connected to the circuit breaker, the other end of the cable was either (i) connected to the 480 VAC motor, or (ii) open ended (disconnected from the motor). FDR and SSTDR measurements were made from the control box (circuit breaker) end of the cable. For consistency between open ended and motor-connected test conditions, FDR and SSTDR measurements were made with the cable de-energized.

4.1.1 Shielded Cable

Figure 4-2 shows the results of FDR and SSTDR measurements on the shielded cable when connected to and disconnected from a motor. Both SSTDR and FDR responses show large peaks and troughs corresponding to the start and end of the cable (at 0 ft and 88 ft). Neither the FDR nor the SSTDR showed any substantial difference except near the cable end based on the presence or absence of the motor. The SSTDR energized and de-energized plots connected to the motor were also quite identical.

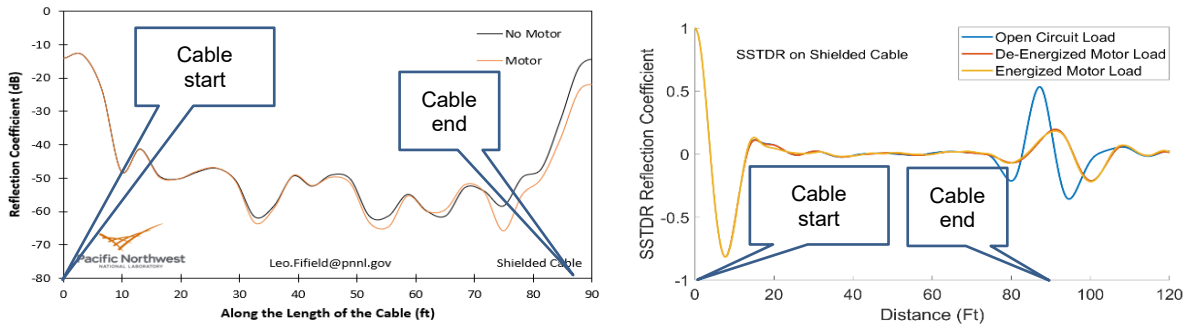

Figure 4-2. (Left) FDR and (right) SSTDR reflection coefficient magnitude as a function of cable length with the motor connected and disconnected and for SSTDR- energized for the shielded cable.

4.1.2 Non-Shielded Cable

Figure 4-3 illustrates the FDR and SSTDR responses for the non-shielded cable when connected to and disconnected from a motor. As in the case of the shielded cable, both SSTDR and FDR responses show

large peaks corresponding to the start and end of the cable (at 0 ft and 88 ft), and neither the FDR nor the SSTDR showed any affect for the presence or absence of the motor. The SSTDR energized and de-energized plots were also quite identical.

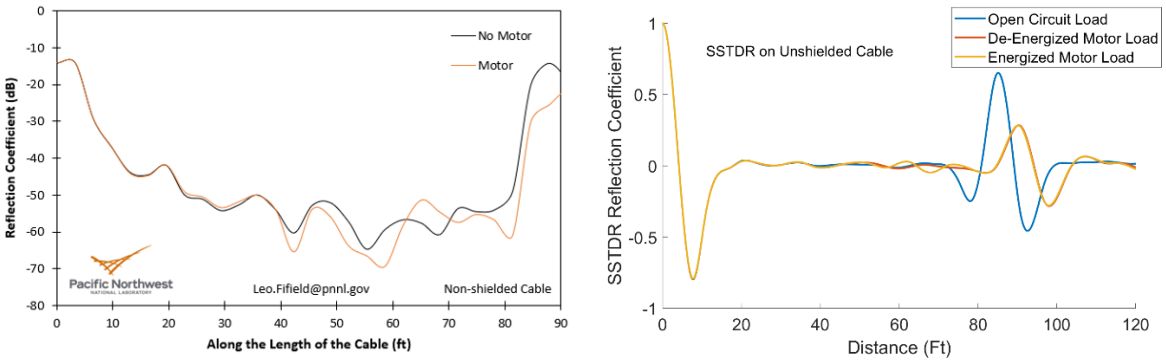

Figure 4-3. (Left) FDR and (right) SSTDR reflection coefficient magnitude as a function of cable length with the motor connected (and disconnected) and for SSTDR- energized for the non-shielded cable.

4.2 Ground Fault and Short Circuit Fault Detection

Electrical faults are some of the most common anomalies experienced by cables in service. While ground faults are detected when the cable is energized and the current takes an unexpected path to ground, short circuit (line-to-line) occurs when two lines of the circuit that are intended to be at different voltage have an abnormal connection. Both fault conditions are potentially dangerous. Timely detection and mitigation is valuable for safe long term operation of cable systems. In this work, the effectiveness of SSTDR to detect ground faults and short circuit faults in an energized cable was evaluated. For the test scenarios described below, SSTDR measurements were made to study electrical fault detection performance. First, the results for ground faults are presented followed by those for the short circuit faults.

4.2.1 Ground Fault

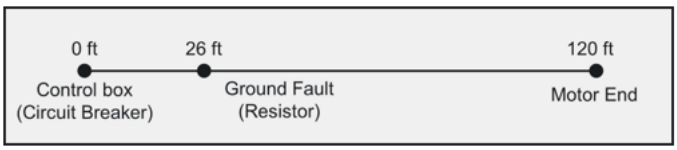

Figure 4-4. Schematic representation of the cable route for ground fault testing.

To perform ground fault measurements, a non-inductive, high-power resistor was introduced in the cable pathway to allow for a large draw of current from the live conductor to ground. A new and slightly longer cable segment (120-ft.) was used instead of the 88-ft. cable from previous tests. Prior to attachment of the resistor, a baseline SSTDR measurement was made on the cable. Following this, three ground fault test scenarios were implemented using 312 Ω, 400 Ω, and 675 Ω resistors, respectively, and SSTDR measurements were taken for each of these scenarios. A schematic representation of the cable routing pathway and ground fault location is given in Figure 4-4.

Figure 4-5 shows the results of ground fault detection studies conducted on the energized non-shielded cable using SSTDR. In the raw SSTDR data (prior to baseline correction), a sharp peak corresponding to the start (circuit breaker end) of the cable was observed at 0 ft, while another prominent peak was observed at 120 ft corresponding to the motor-end of the cable. The evaluated ground fault (located at 23 ft) for all three scenarios was not directly observable by SSTDR, with or without baseline correction. Further

investigation may allow for development of this technology to produce larger amplitude changes in response to ground faults.

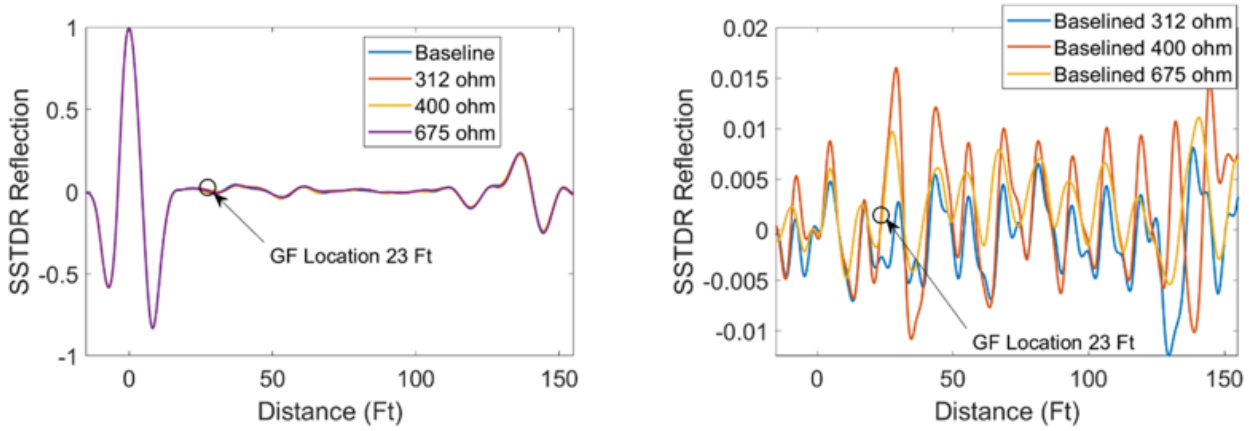

Figure 4-5. Ground fault detection by SSTDR before (left) and after (right) baseline correction.

4.2.2 Short Circuit Fault

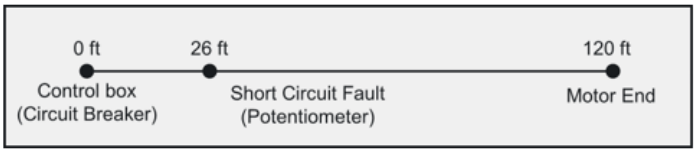

Figure 4-6. Schematic representation of the cable route for short circuit fault testing.

For short circuit faults, a capacitor-coupled potentiometer was used to introduce a short circuit fault between two of the conducting leads of the cable. First, a baseline SSTDR measurement of the cable was obtained without the potentiometer connected. Next, SSTDR measurements were collected for four potentiometer settings including 0 Ω (short circuit, SC), 312 Ω, 1 kΩ, and 2 kΩ. A schematic representation of the cable routing pathway and short circuit fault location is given in Figure 4-6.

In Figure 4-7, the SSTDR response for short circuit faults in the non-shielded cable is shown with and without baseline correction. Similar to the ground fault measurements, prior to baseline correction the circuit breaker end and the motor end of the cable correspond to the two peaks at 0 ft and 120 ft, respectively. The SC fault located at 26 ft corresponds to the trough in the SSTDR response. The change in the magnitude of the SSTDR reflected signal is largest when the potentiometer was set to 0 Ω (i.e., a short circuit). The magnitude of the reflected response at 26 ft decreases as the potentiometer setting increases to 2 kΩ. This trend is clearly apparent both before and after baselining. Within the scope of this report, short circuits were strongly detected using the SSTDR measurement technique.

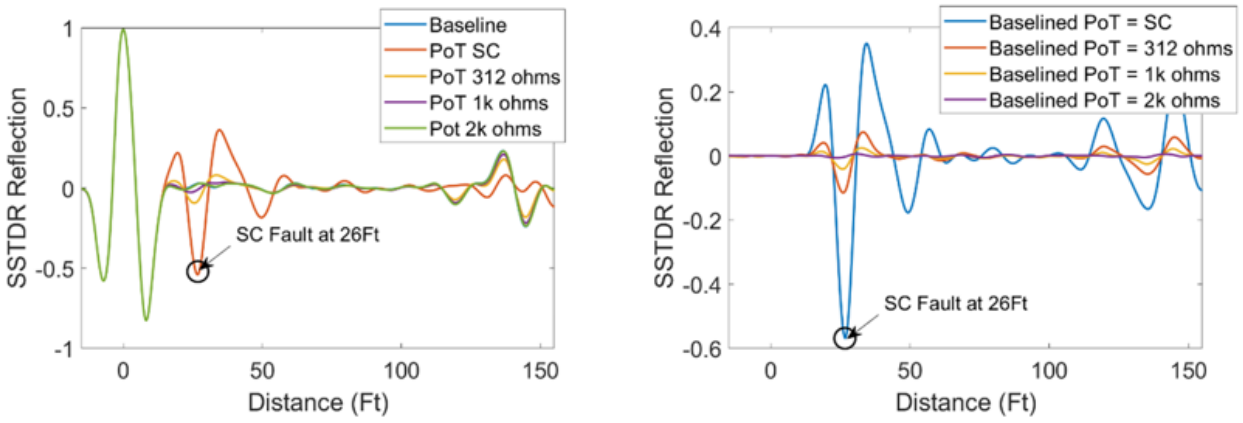

Figure 4-7. Short circuit fault detection by SSTDR before (left) and after (right) baseline correction.

4.3 Water Ingress Fault Detection

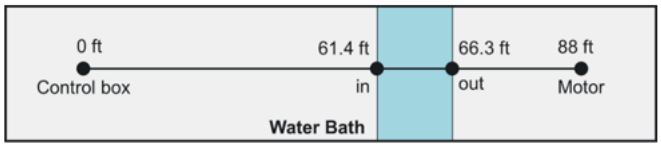

Figure 4-8. Schematic representation of the cable route and water bath location for water ingress testing.

To evaluate the effectiveness of FDR and SSTDR for the presence or absence of water and water ingress faults in both shielded and non-shielded cables, a series of water test conditions were designed and investigated in the PNNL ARENA cable test bed. FDR and SSTDR measurements were made for each test condition to compare the performance of the online SSTDR technique in comparison with offline FDR in pinpointing and resolving water ingress defects. For this purpose, an 88-ft long cable was routed from the control panel (circuit breaker), through the water bath, and to the 480 VAC motor as shown in the schematic representation in Figure 4-8. Both shielded and non-shielded cables were evaluated using an identical test setup. As shown, 4.5 ± 0.5 ft of the cable was routed through a basin located between 61.4 ± 0.2 ft and 66.3 ± 0.3 ft from the control box end of the cable. To wet the cable, water was pumped into the basin until the cable was completely submerged. With this overall test setup, the test conditions that were implemented to obtain the results discussed in this report are described below in Table 2.

Table 2. Test conditions implemented for water ingress tests.

Test Number	Cable Condition			Test Description
	Wet/Dry	Jacket Damage*	Insulation Damage	
1	Dry	No	No	Baseline test on dry cable
2	Wet	No	No	Baseline test on wet cable
3	Dry	Yes	No	Dry cable with jacket damage
4	Wet	Yes	No	Wet cable with jacket damage
5	Wet	Yes	Yes	Wet cable with one insulation damaged
6	Wet	Yes	Yes	Wet cable with two insulations damaged
7	Wet	Yes	Yes	Wet cable with three insulations damaged

*Shield removed during jacket removal process.

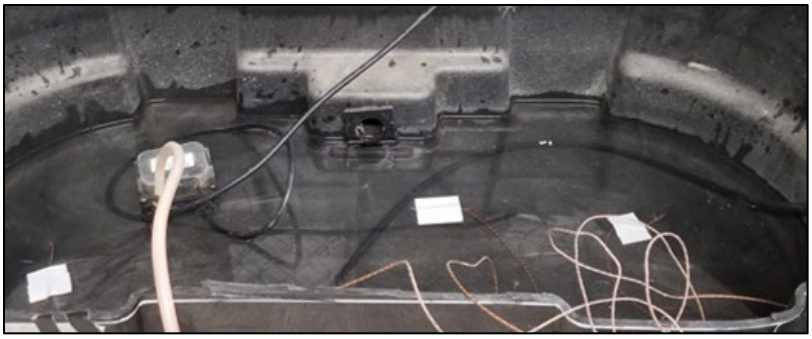

Figure 4-9. Non-damaged cable submerged in water bath.

4.3.1 No Cable Damage

Water detection (jacket submerged or dry) was evaluated for shielded and non-shielded cables with no damage. Figure 4-10 shows the FDR response at 500 MHz for the intact shielded and non-shielded cables in dry and wet conditions. The results show no clearly distinguishable peaks observed in the water bath region for the wet shielded cable, while two peaks seemingly corresponding to the cable entry to and exit from the water were observed for the non-shielded cable. Consequently, when the cables were not damaged, FDR was successful in detecting water for the non-shielded cable but did not effectively detect water for the shielded cable. These results are consistent with prior studies on similar cables (Glass S.W. et al., 2021).

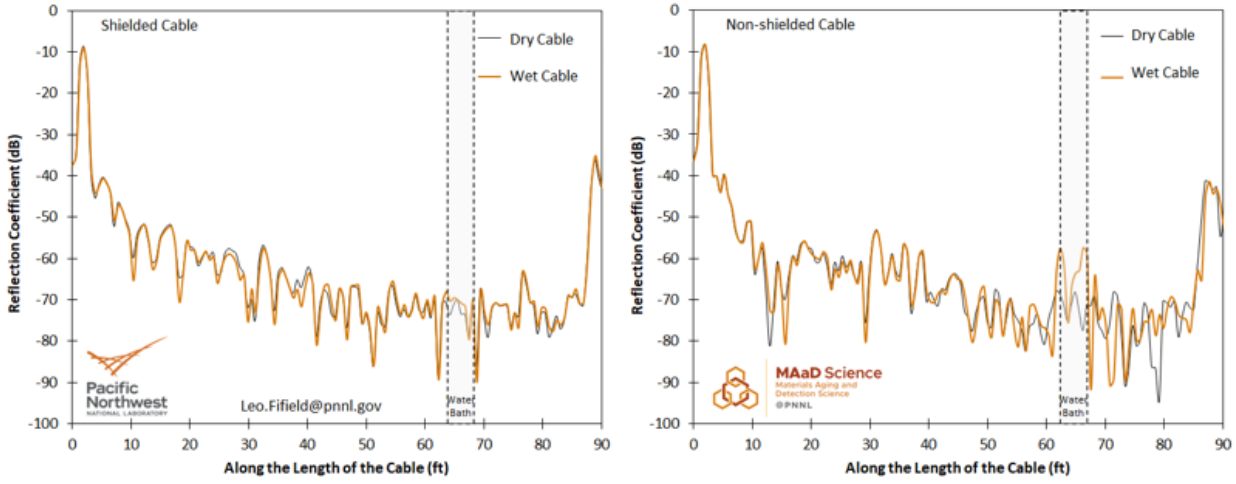

Figure 4-10. FDR reflection coefficient of dry and wet shielded and non-shielded cables at 500 MHz.

Both shielded and non-shielded cables with no damage were energized and SSTDR measurements were taken to detect moisture. Figure 4-11 shows the SSTDR reflection coefficient for the energized shielded and non-shielded cables. Similar to the FDR response, no clearly distinguishable peaks were observed in the water bath region for the wet shielded cable, whereas for the non-shielded cable two peaks likely corresponding to the entry and exit points of the water bath were observed in the wet signal. The overall noise level for this SSTDR makes definitive conclusions on water detection challenging.

In conclusion, both FDR and SSTDR signals showed similar success in detecting moisture exposure for intact non-shielded cables. However, neither technique showed detectable responses for moisture presence/absence or entry/exit to and from the water bath in shielded cables.

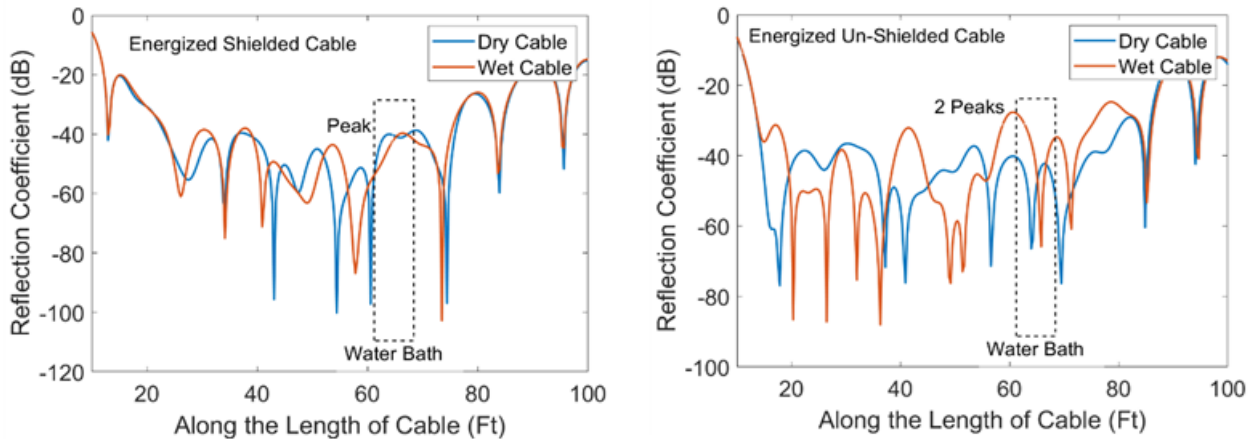

Figure 4-11. SSTDR reflection coefficient for dry and wet energized (left) shielded and (right) unshielded cables.

4.3.2 Jacket (and Shield) Damage

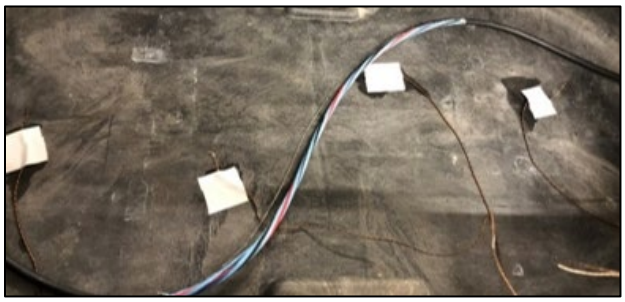

Figure 4-12. Damaged 2-ft section of the dry shielded cable with jacket and shield removed to expose insulated wires.

A 2-ft section of the jacket (for the non-shielded cable) and a 2-ft section of the jacket and shield (for the shielded cable) were removed from the middle of the submerged (water bath) section of the cable as shown in Figure 4-12. Under dry conditions (no water present in the water bath), the FDR response to jacket (and shield) damage at 500 MHz was examined. The results of this test are shown in Figure 4-13 below. Large peaks corresponding to the location of the damaged region were observed in the FDR response for both shielded and non-shielded cables. Edge resolution of the damaged region was better for the shielded cable as compared to the non-shielded cable.

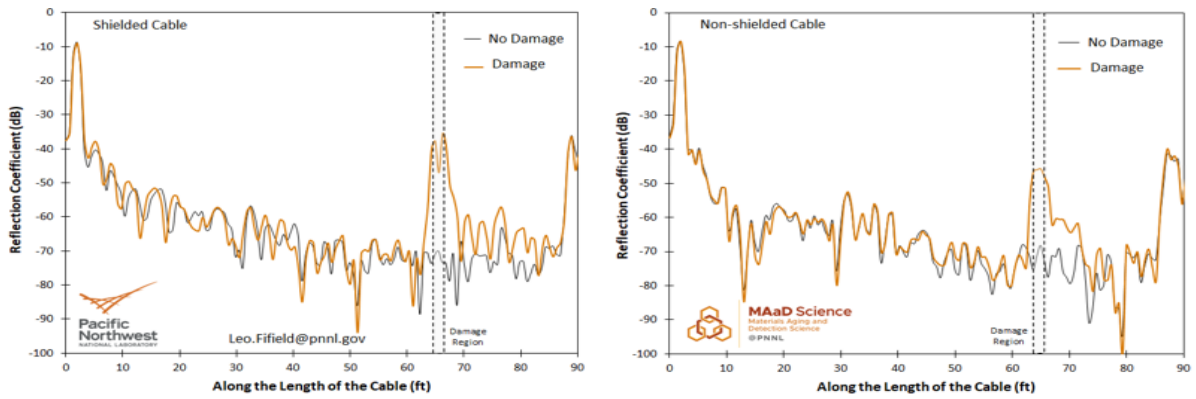

Figure 4-13. FDR reflection coefficient at 500 MHz under dry conditions for shielded cable (left) with 2-ft section of jacket and shield removed and, non-shielded cable (right) with 2-ft section of jacket removed.

Corresponding measurements on the shielded and non-shielded cables under dry conditions with jacket (and shield) damage were performed using SSTDR. The results of these measurements are shown in Figure 4-14. The peak amplitude in the reflection coefficient was found to be approximately 15 dB greater in the damaged region for the shielded and non-shielded cables as compared to that of the respective undamaged cables in the same region. Although this increase in the SSTDR response peak is similar to the trend observed in FDR, it was observed that the relative change in the FDR response between the undamaged and damaged cables was larger and more easily detected by FDR as compared to SSTDR. Therefore, using FDR it was easier to identify and pinpoint the location of the damaged section as an anomaly in the cable response as compared to SSTDR.

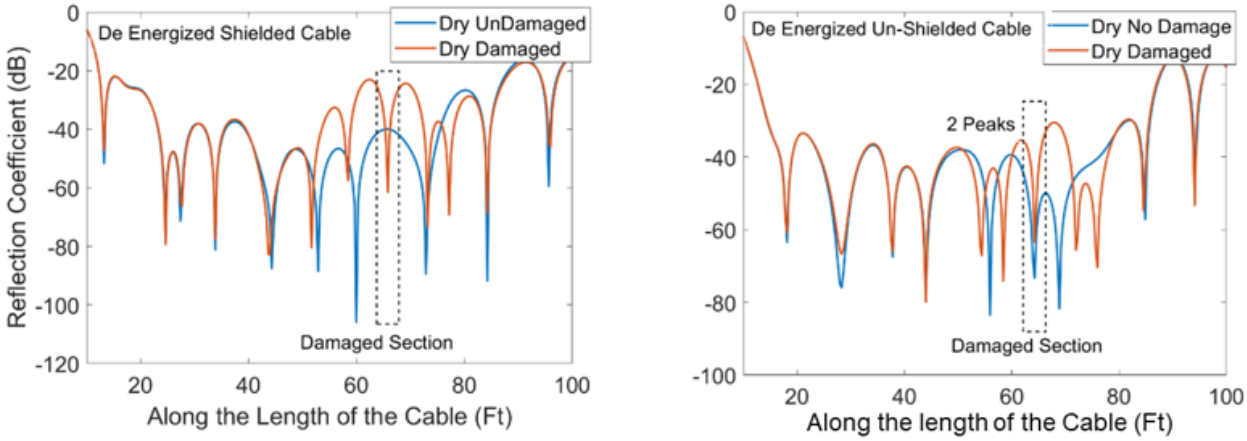

Figure 4-14. SSTDR reflection coefficient under dry conditions for shielded cable (left) with 2-ft section of jacket and shield removed and, non-shielded cable (right) with 2-ft section of jacket removed.

4.3.3 Insulation Damage

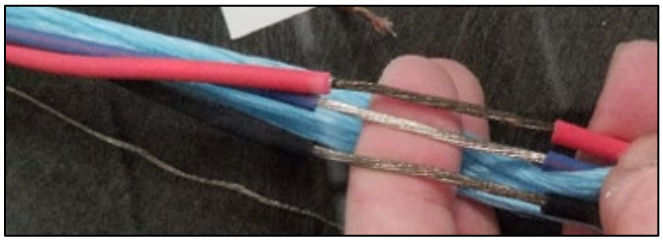

Figure 4-15. Insulation removed from 2-inch section of wires to expose the copper conductors within.

At the midpoint of the damaged, submerged section of the cable (with 2-ft of jacket and/or shield removed), a 2-inch segment of the insulation was excised from the three wires to expose the conductors within as shown in Figure 4-15. The wet FDR responses at 500 MHz for the shielded and non-shielded cables with insulation damage are shown as compared to those of the dry undamaged cable in Figure 4-16. It was observed that for both the shielded and non-shielded cables, strong and clearly distinguishable impedance changes were observed in the form of multiple sharp peaks in the region with insulation damage and jacket damage. The large change in reflection coefficient may be further attributed to the direct exposure of the conductors to water. The results show that when the appropriate frequency bandwidth (i.e., 500 MHz) was chosen, the FDR technique could effectively detect the location of water ingress faults within shielded and non-shielded cables. Moreover, it must be noted that the FDR response in the water bath region for both the shielded and non-shielded cables was fairly complex with multiple sharp peaks. Further investigation is required to resolve the peaks corresponding to the physical changes within the cable and the test environment.

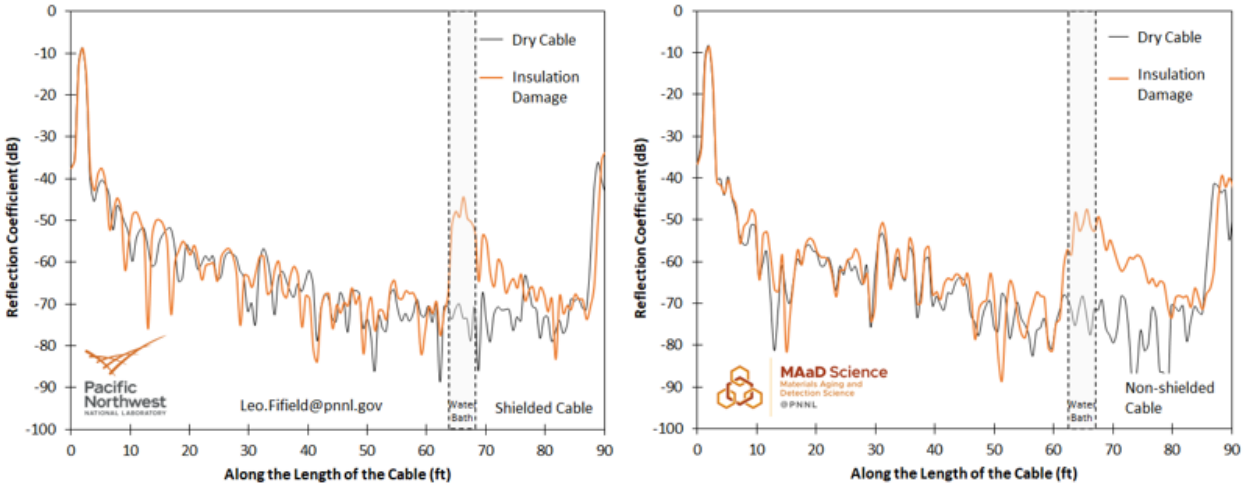

Figure 4-16. FDR reflection coefficient at 500 MHz under wet conditions for shielded (left) and non-shielded (right) cables with 2-inch section of insulation removed as compared to the 500 MHz response of the corresponding dry, undamaged cable.

When evaluating water ingress faults on the cables using SSTDR, the reflection coefficients for the progressive damage tests were plotted against the length of the cable to evaluate the change in the SSTDR response in accordance with changes in the cable as shown in Figure 4-17. As seen in the figure, starting with the intact cable (dry, no damage), the SSTDR response in the region of interest (water bath and damaged section) showed progressive increase in peak intensity as a function of increasing damage to the cable even when energized. However, as noted in the previous case, the change in the SSTDR response, although discernable, was not strongly pronounced in proportion with the severity of damage to the cable (conductor exposed to water). Further improvements to the resolution and sensitivity of the SSTDR technique may help amplify drastic impedance discontinuities in the cable.

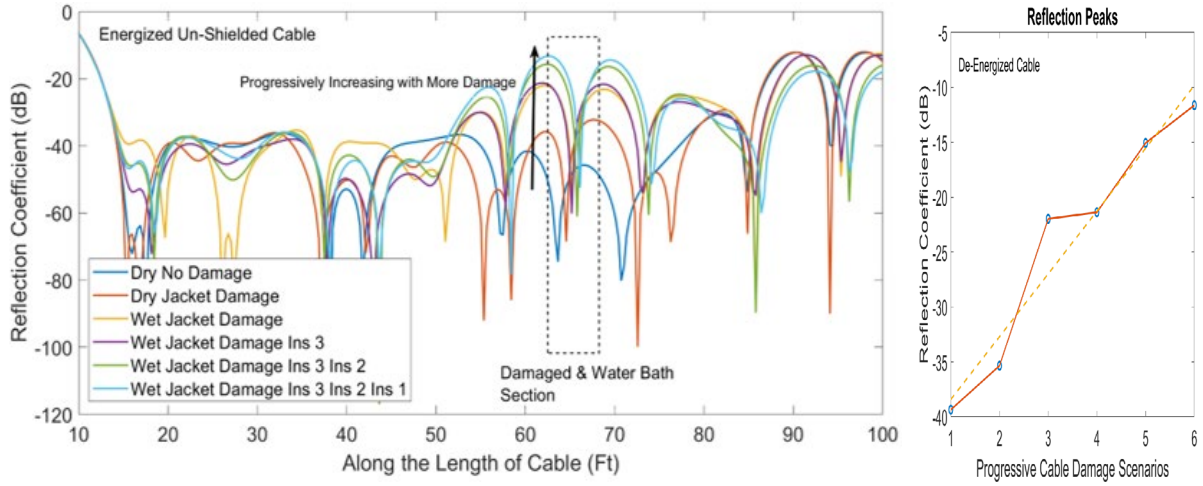

Figure 4-17. SSTDR reflection coefficient under dry and wet conditions for the energized non-shielded cable (left) with progressive damage under dry and wet conditions (right).

4.4 Accelerated Thermal Aging Detection

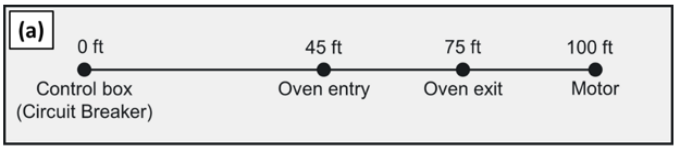

Figure 4-18. Schematic representation of the cable route for accelerated thermal aging testing.

Accelerated thermal aging in an air-circulating oven at high temperature was selected to induce thermal degradation representative of long-term aging in a non-shielded cable. FDR and SSTDR measurements were made periodically during the aging timeline to evaluate the progression of degradation in the cable. Figure 4-18 shows a schematic representation of the cable routing pathway, while Figure 4-19 shows the overall test setup.

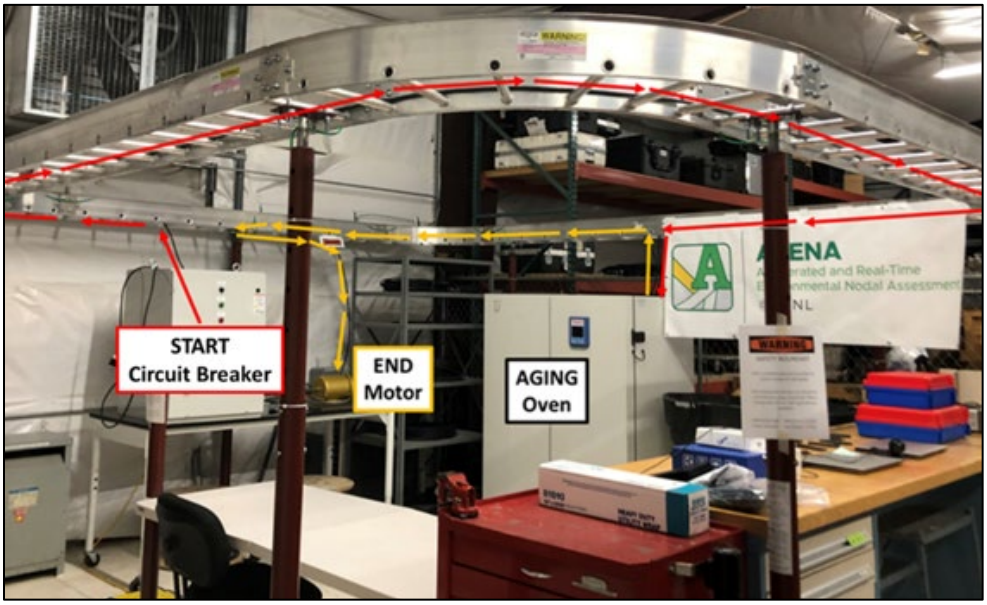

Figure 4-19. Overall test setup for accelerated thermal aging.

The 100 ft long cable was routed from the circuit breaker (START) through the overhead cable trays to an air-circulating oven (ThermoFisher Scientific HerathermTM OMH-750 Advanced Protocol) where a 30 ft section was carefully wrapped around a glass mandrel and routed out of the oven and finally to a 480 VAC motor on the other end. As shown in Figure 4-20, inside the oven, insulation straw samples serving as cable witness specimens were placed alongside the aging 100 ft cable to track mechanical property changes as a function of aging time. These samples were prepared prior to aging – the wires from within the unaged cable were removed and the conductors were extracted – to be aged alongside the cable for up to 62 days. Accelerated isothermal aging was performed on the 30 ft cable section and the insulation straw samples at 140°C. FDR and SSTDR measurements were performed on the entire cable at 0, 3, 7, 11, 15, 19, 23, 27, 33, 37, 43, 49, 55, and 62 days of aging time. At each of the corresponding aging time points, insulation straw samples were removed from the oven and mechanical tensile tests were performed to track insulation degradation. FDR measurements were conducted on the de-energized cable, while SSTDR measurements were taken when the cable was energized. Further, for each aging time point, FDR and SSTDR measurements were made at ambient (approximately 22°C; oven off) and 140°C (oven on) to evaluate the influence of measurement temperature on aging detection. To accomplish this, the oven and motor power were periodically shut down (at the aging time points) to de-energize the cable and to allow it

to cool down to room temperature to make measurements under ambient conditions. Once measurements were completed, the oven and motor were restarted to resume aging.

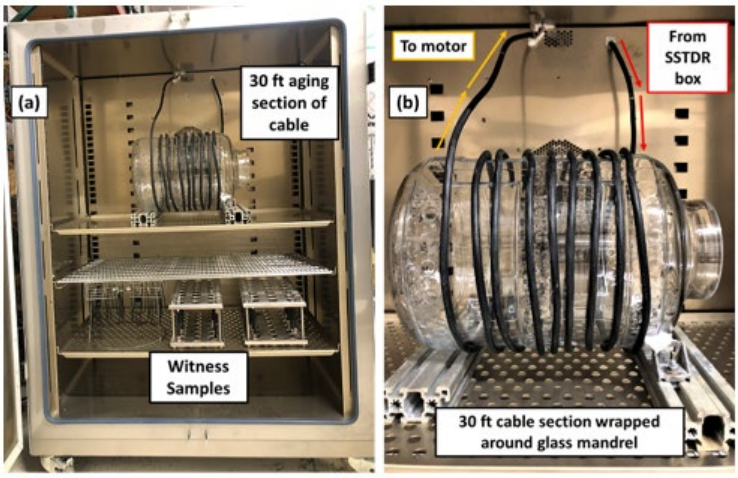

Figure 4-20. (a) Cable and witness samples inside oven and (b) enlarged image of cable wrapped around mandrel inside oven.

4.4.1 Mechanical Property Correlation

The destructive test gold standard for accelerated aging cable service life is the elongation at break (EAB, also known as strain at break) mechanical tensile test. To quantify the extent of insulation degradation as a function of accelerated thermal aging at 140°C, mechanical tensile tests were performed on insulation straw specimens at progressive aging time points to obtain EAB properties of the insulation material. The percentage change in the EAB plotted as a function of aging time on a logarithmic scale is reported in Figure 4-21. The results showed that the mechanical response of the EPR insulation remained nearly constant for up to 37 days of aging, following which a sharp drop was observed in the strain at break from 43 to 62 days of aging. The long induction period for changes in mechanical properties suggests that the EPR insulation exhibits resilience to thermal degradation at 140°C. Moreover, FDR measurement detected changes within the cable at as early as 19 days of aging, which illustrates the high sensitivity of this technique in detecting cable aging as compared to mechanical benchmark tests.

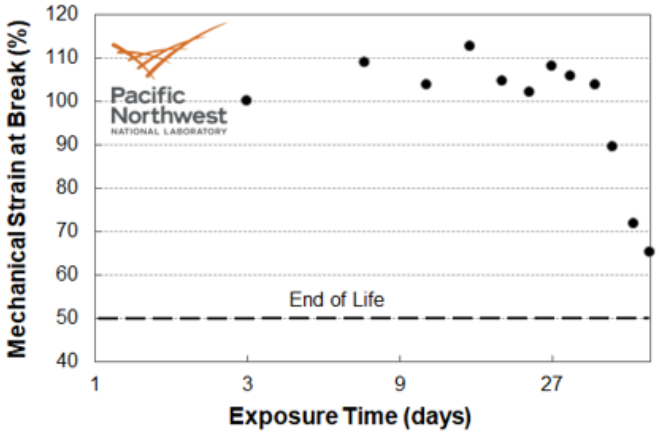

Figure 4-21. Percentage change in mechanical strain at break (EAB) as a function of aging time for EPR insulation.

4.4.2 Frequency Domain Reflectometry (FDR)

Figure 4-22 shows the magnitude of the reflected FDR signal converted to the time domain for ambient (22°C) and 140°C measurement temperatures plotted against cable length for all aging time points. Across all aging time points and both measurement temperatures, large peaks corresponding to the two ends of the cable were observed at 0 ft and 100 ft (i.e., circuit breaker at 0 ft and motor at 100 ft). In the test setup, cable entry into the oven was at 45 ft and exit was at 75 ft (see Figure 4-23 for corresponding reflection coefficients). First, at ambient conditions, the oven exit peak shows a sharp rise at 3 days and then increases steadily with increasing aging time, while the oven entry peak stays constant up to 15 days and then exhibits a similar rising trend. Given there are no temperature effects at ambient conditions, the changes observed in the magnitude of oven entry and exit peaks may be attributed to thermal degradation of the cable as a function of aging time. Next, for measurements at 140°C, the reflected peaks were detected at the points of cable entry and exit, to and from the oven. However, the peak magnitude is lower than those measured at corresponding aging times under ambient conditions. Further, for up to 31 days, the oven exit peak remains constant, while the oven entry peak first decreases up to 15 days and then gently rises for up to 62 days. This contrast between the ambient and 140°C oven response for equivalent aging time points of the cable was somewhat surprising but illustrates the importance of measurement temperature for electrical reflectometry.

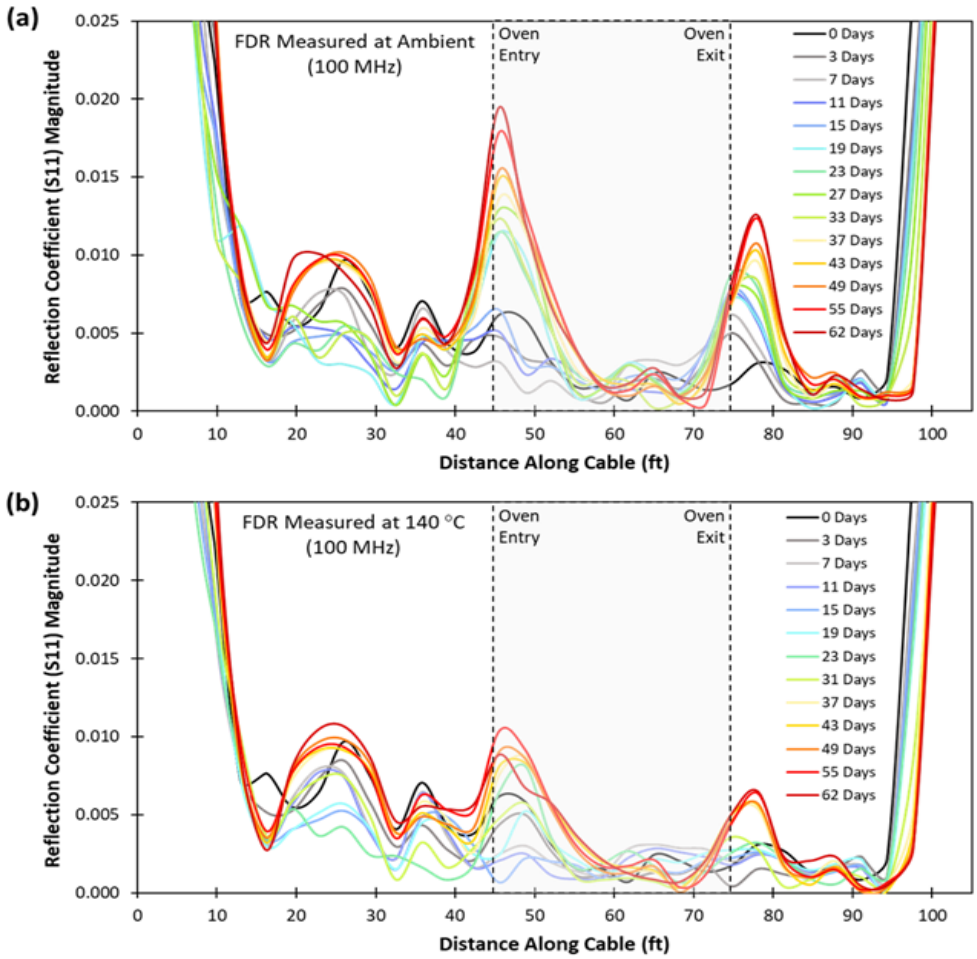

Figure 4-22. FDR Reflection coefficient of the de-energized non-shielded cable as a function of cable length for (a) ambient, and (b) at 140°C measurement temperatures.

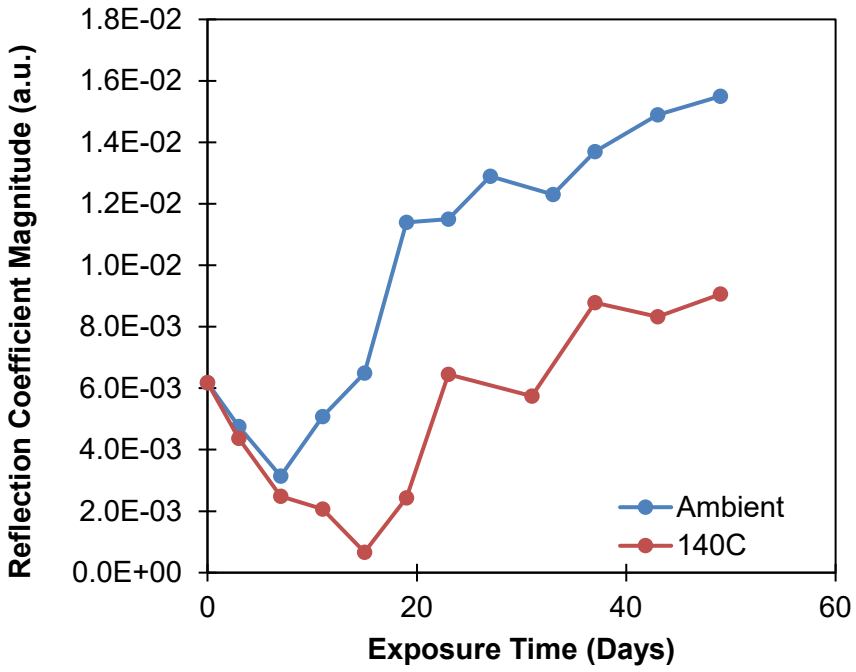

Figure 4-23. Thermal aging oven entrance peak trend over 49 days. (This plot made before data was available for day 55 and 62).

4.4.3 Spread Spectrum Time Domain Reflectometry (SSTDR)

As in the case of FDR, SSTDR measurements were taken at each of the cable aging time points, with the key difference being that the cable was energized for SSTDR. Furthermore, the reflection coefficient magnitude was computed for the SSTDR reflected signal using an identical approach to the FDR data processing for a direct comparison. The results of the SSTDR measurements taken at ambient and 140°C measurement temperatures for all the aging time points of the cable are shown in Figure 4-24 and Figure 4-25. Note that SSTDR data was only taken through 55 days rather than 62 days of aging.

It was observed that, similar to the FDR response, the oven entrance and exit peaks at 45 ft and 75 ft respectively show changes in magnitude as a function of aging time. Although, at both ambient and 140°C measurement conditions, there is no clearly apparent trend in the magnitude of oven entry or exit peaks. At ambient conditions, the oven entry peak magnitude shows a slight increase after 19 days of aging and then plateaus for up to 49 days. One the other hand, at 140°C it is challenging to distinguish the various aging time points from one another due to large overlap between the traces. While SSTDR was able to detect the oven entry and exit points of the cable, clear trends with aging were not strongly evident in the data. This may be attributed to the poor spatial resolution achieved at 24 MHz frequency. Higher frequency bandwidths with better spatial resolution may improve the performance of SSTDR in aging detection. In contrast, FDR with the higher bandwidth showed clear trends with cable aging and degradation in this report.

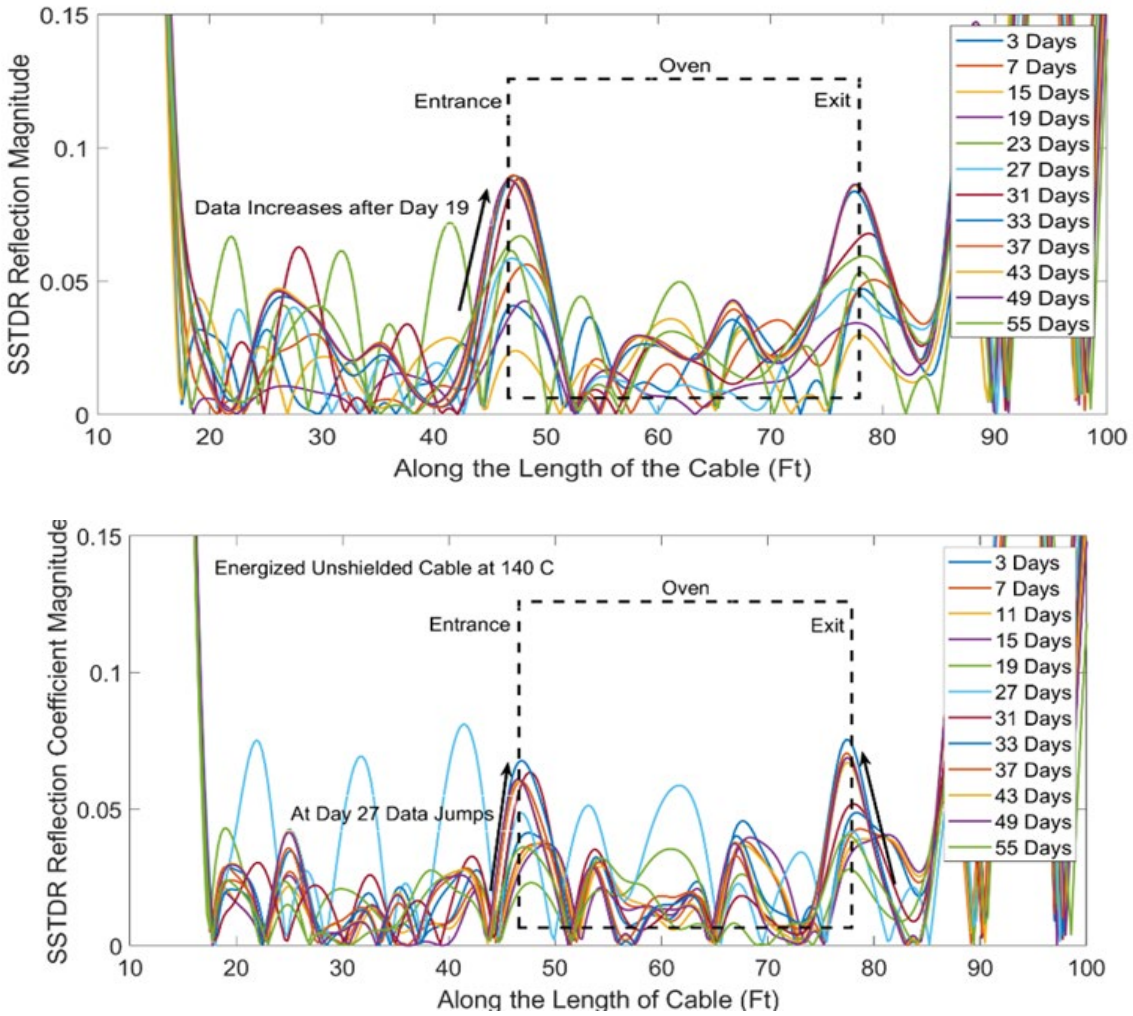

Figure 4-24. SSTDR Reflection coefficient of the energized non-shielded cable as a function of cable length for (a) ambient, and (b) 140°C measurement temperatures.

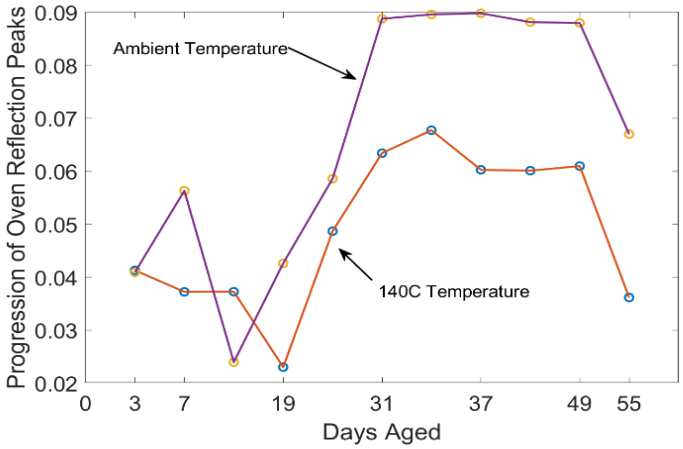

Figure 4-25. The SSTDR oven entrance reflection magnitude peaks for ambient temperature (purple) and at 140C (orange).

5. Observations and Conclusions

The ARENA test bed supported quick evaluation of cables by FDR and SSTDR analysis for several different configurations in a controlled environment. Conclusions and observations are shown below.

1. FDR and SSTDR spectra were equivalent with and without a motor being connected for both the shielded and non-shielded case.
2. SSTDR was unable to detect ground faults but was able to detect short circuit (line-to-line) faults with varying resistances along the cable.
3. For all anomaly detection tests, the SSTDR signal was not significantly different between unenergized and energized cables. FDR was not performed on energized cable.
4. Both FDR and SSTDR were able to show the presence of water for the undamaged non-shielded cable. FDR data taken at 500 MHz bandwidth demonstrated remarkable peaks at the position corresponding to the water bath location along the cable. The SSTDR showed a single peak for the cable section in the water trough. The spatial resolution of the SSTDR may be insufficient to resolve entry and exit from the water bath.
5. Neither the FDR nor the SSTDR showed any indication of the presence or absence of water for the undamaged shielded cable.
6. Mechanically damaged cable jackets and insulation in both shielded and unshielded cables were detectable by FDR and SSTDR. When the mechanically damaged cable was exposed to water detectability improved and the peak broadened – possibly because the water wicked into the cable through the damaged shield and insulation.
7. Both FDR and SSTDR were able to detect progressive thermal aging of the shielded cable. The SSTDR peak within the spectra increased slightly with aging time when measured at ambient conditions then plateaued after approximately 31 days. On the other hand, sharp FDR spectral peaks at oven entry and exit were observed to increase steadily with aging time up to 62 days when measured at ambient conditions.
8. Contrary to expectation, FDR and SSTDR measurements at ambient conditions on the thermally aged cables showed larger changes in peak magnitude as compared to measurements taken at 140°C.
9. The thermal aging was benchmarked with EAB measurements which showed a sharp decline after 42 days and up to 62 days but did not reach 50% of initial EAB criteria, often designated as end of useful life for the cable.

11 The trend behavior was different between the EAB values, the FDR peaks, and the SSTDR peaks.

12. Both FDR and SSTDR are subject to frequency bandwidth effects that influence the spectral peaks and the spatial resolution of the measurements. FDR data was typically taken at 0.1, 0.5, and 1.0 MHz bandwidth. The SSTDR data was fixed at a bandwidth of 48 MHz. Such a low frequency bandwidth may be preferable for interrogating longer cable lengths but did not serve well for resolving the cable anomalies in this study. This bandwidth was not an adjustable parameter of the standard instrument but may be considered as a future instrument upgrade by Livewire Innovations, Inc.

6. References

Agilent. 2012. *Time Domain Analysis Using a Network Analyzer.* Agilent Technologies, Santa Clara, California

Copper_Mountain. 2020. "TR1300/1 2-Port 1.3 GHz Analyzer." accessed 08/29/2022. https://coppermountaintech.com/vna/tr1300-1-2-port-1-3-ghz-analyzer/.

Fifield, L S, M P Westman, A Zwoster, and B Schwenzer. 2015. *Assessment of Cable Aging Equipment, Status of Acquired Materials, and Experimental Matrix at the Pacific Northwest National Laboratory.* Pacific Northwest National Laboratory, Richland, Washington

Furse, C., Chung You Chung, R. Dangol, M. Nielsen, G. Mabey, and R. Woodward. 2003. "Frequency-domain Reflectometry for On-board Testing of Aging Aircraft Wiring." *IEEE Transactions on Electromagnetic Compatibility* 45 (2):306-315. doi: 10.1109/TEMC.2003.811305.

Glass, S W, A M Jones, L S Fifield, and T S Hartman. 2016. *Distributed Electrical Cable Non-Destructive Examination Methods for Nuclear Power Plant Cable Aging Management Programs.* Pacific Northwest National Laboratory, Richland, WA

Glass, S W, A M Jones, L S Fifield, T S Hartman, and N Bowler. 2017. *Physics-Based Modeling of Cable Insulation Conditions for Frequency Domain Reflectometry (FDR).* PNNL-26493, Pacific Northwest National Laboratory, Richland, Washington

Glass S.W., L.S. Fifield, G. Dib, J.R. Tedeschi, A.M. Jones, and T.S. Hartman. 2015. *State of the Art Assessment of NDE Techniques for Aging Cable Management in Nuclear Power Plants FY2015.* Pacific Northwest National Laboratory, Richland, Washington

Glass S.W., Spencer M.P., Sriraman A., Fifield L.S., and Prowant M. 2021. *PNNL-31934 Nondestructive Evaluation (NDE) of Cable Moisture Exposure using Frequency Domain Reflectometry (FDR).* Pacific Northwest National Laboratory,

Glass, S.W., L S. Fifield, and M Prowant. 2021. *PNNL 31415 PNNL ARENA Cable Motor Test Bed Update.*

Glass, S.W., L.S. Fifield, and N. Bowler. 2020. *PNNL 155612 Cable Nondestructive Examination Online Monitoring for Nuclear Power Plants.* Pacific Northwest National Laboratory, Richland Washington

Glass S.W., Spencer M.P., Sriraman A., Fifield L.S., Prowant M. 2021. *PNNL 31934 Nondestructive Evaluation (NDE) of Cable Moisture Exposure using Frequency Domain Reflectometry (FDR).* Richland Wa

Glass, Samuel W., Anthony M. Jones, Leonard S. Fifield, Nicola Bowler, Aishwarya Sriraman, and Roberto Gagliani. 2018. *Dielectric Spectroscopy for Bulk Condition Assessment of Low Voltage Cable -- Interim Report.* PNNL-27982 United States 10.2172/1491578 PNNL English, ; Pacific Northwest National Lab. (PNNL), Richland, WA (United States),

IEEE. 2019. "IEEE/IEC International Standard - Nuclear power plants -- Instrumentation and control important to safety -- Electrical equipment condition monitoring methods - Part 6: Insulation resistance." *IEC/IEEE 62582-6:2019*:1-52. doi: 10.1109/IEEESTD.2019.8877510.

Naik S., Furse C.M., Boroujeny B.F. . 2006. "Multicarrier Reflectometry." *IEEE Sensors Journal* 6 (3): 812-818.

NRC. 2021. "Status of Subsequent License Renewal Applications." NRC, accessed 09/16/2021. https://www.nrc.gov/reactors/operating/licensing/renewal/subsequent-license-renewal.html

Simmons, K L, P Ramuhalli, D L Brenchley, and J B Coble. 2012. *Light Water Reactor Sustainability (LWRS) Program – Non-Destructive Evaluation (NDE) R&D Roadmap for Determining Remaining Useful Life of Aging Cables in Nuclear Power Plants.* Pacific Northwest National Laboratory, Richland, Washington

Smith P., Furse C., Kuhn P. 2008. "Intermittent Fault Location on Live Electrical Wiring Systems." *SAE International*.

Tsai P., Chung Y. Lo C., Furse C. 2005. "Mixed Signal Reflectometer Hardware Implementation for Wire Fault Location." *IEEE Sensors Journal* 5 (6):1479-1482.